



Published in final edited form as:

*Cell Mol Bioeng.* 2009 September 1; 2(3): 405–415. doi:10.1007/s12195-009-0075-5.

## A Trabecular Bone Explant Model of Osteocyte–Osteoblast Co-Culture for Bone Mechanobiology

Meilin Ete Chan<sup>1</sup>, Xin L. Lu<sup>1</sup>, Bo Huo<sup>1,2</sup>, Andrew D. Baik<sup>1</sup>, Victor Chiang<sup>1</sup>, Robert E. Guldberg<sup>3</sup>, Helen H. Lu<sup>4</sup>, and X. Edward Guo<sup>1</sup>

<sup>1</sup>Bone Bioengineering Laboratory, Department of Biomedical Engineering, Columbia University, 351 Engineering Terrace, Mail Code 8904, 1210 Amsterdam Avenue, New York, NY 10027, USA

<sup>2</sup>Institute of Mechanics, Chinese Academy of Sciences, Beijing 100080, P.R. China

<sup>3</sup>Institute for Bioengineering and Bioscience, Georgia Institute of Technology, Atlanta, GA 30332, USA

<sup>4</sup>Biomaterials and Interface Tissue Engineering Laboratory, Department of Biomedical Engineering, Columbia University, New York, NY 10027, USA

### Abstract

The osteocyte network is recognized as the major mechanical sensor in the bone remodeling process, and osteocyte–osteoblast communication acts as an important mediator in the coordination of bone formation and turnover. In this study, we developed a novel 3D trabecular bone explant co-culture model that allows live osteocytes situated in their native extracellular matrix environment to be interconnected with seeded osteoblasts on the bone surface. Using a low-level medium perfusion system, the viability of *in situ* osteocytes in bone explants was maintained for up to 4 weeks, and functional gap junction intercellular communication (GJIC) was successfully established between osteocytes and seeded primary osteoblasts. Using this novel co-culture model, the effects of dynamic deformational loading, GJIC, and prostaglandin E<sub>2</sub> (PGE<sub>2</sub>) release on functional bone adaptation were further investigated. The results showed that dynamical deformational loading can significantly increase the PGE<sub>2</sub> release by bone cells, bone formation, and the apparent elastic modulus of bone explants. However, the inhibition of gap junctions or the PGE<sub>2</sub> pathway dramatically attenuated the effects of mechanical loading. This 3D trabecular bone explant co-culture model has great potential to fill in the critical gap in knowledge regarding the role of osteocytes as a mechano-sensor and how osteocytes transmit signals to regulate osteoblasts function and skeletal integrity as reflected in its mechanical properties.

### Keywords

Mechanotransduction; Explant; Osteocytes; Osteoblasts; Gap junction; PGE<sub>2</sub>

### INTRODUCTION

Osteocytes are mature bone cells encased in three-dimensional (3D) mineralized bone matrix. A unique feature of osteocytes is the long dendritic processes (~50  $\mu\text{m}$ ) that travel through canaliculi channels in the extracellular matrix. These processes connect osteocytes in the

lacunae with each other and with other types of cells, such as osteoblasts on the bone surface, to form an extensive cellular communication network.<sup>8</sup> A recent study demonstrated that the absence of osteocytes alone could induce osteoporosis.<sup>35</sup> The transgenic mice with ablated osteocytes were resistant to unloading (tail suspension) induced bone loss, indicating the critical role of osteocytes in detecting the presence or absence of mechanical signals, controlling the bone remodeling process, and maintaining skeleton integrity. *In vitro* cell studies subjecting osteocytes to mechanical stimuli such as fluid shear have identified several important biochemical pathways involved in bone mechanotransduction, such as intracellular calcium, primary cilia, gap junction intercellular communication (GJIC), prostaglandin E<sub>2</sub> (PGE<sub>2</sub>), and nitric oxide.<sup>1,2,21,22,24,34,36</sup> It has also been recognized that direct biochemical pathways between osteocytes or between osteocytes and osteoblasts rely on either direct intercellular contacts such as gap junctions or paracrine/autocrine signaling via the narrow pericellular space between the osteocytic processes and the canalicular wall. Osteocytes have been shown to form gap junctions mainly using connexin 43 (Cx43), which allow rapid communication between two connected cells. In addition, Cx43 has been shown to form unapposed hemi-channels, and these hemi-channels can release PGE<sub>2</sub> and adenosine-5'-triphosphate (ATP) upon mechanical stimulation.<sup>13,19,23</sup> A major limitation in most *in vitro* studies of osteocytes is the disruption of the spatial relationship between osteocytes and osteoblasts, as well as between osteocytes and the mineralized extracellular matrix. For example, it is almost impossible to mimic the *in vivo* 3D canalicular system in these 2D *in vitro* culture systems. Thus, a critical gap in knowledge remains regarding the role of osteocytes as a mechano-sensor and how osteocytes transmit signals to regulate osteoblast functions.

Unlike 2D *in vitro* cell studies, explant cultures of bone tissue have the advantage of allowing live osteocytes to maintain their *in vivo* 3D morphology and intercellular connections and to be surrounded by their native extracellular environment. Explant cultures can also simplify the complexities of *in vivo* animal models, allowing the roles of individual biochemical or mechanical factors to be investigated independently. Such bone explant culture models have been used to study the osteocyte response to various biochemical and mechanical stimuli in their physiological environment, both in cortical and trabecular bone.<sup>9,15-18,20,25,28-30,40</sup> In this study, a novel 3D trabecular bone explant model of a co-culture of osteocytes and primary osteoblasts was developed and characterized. With the ability to sustain long-term culture, the functional bone formation and changes in elastic modulus of trabecular bone were quantitatively assessed. The objectives of this study were to: (1) establish a 3D trabecular bone explant model of a co-culture of osteocytes and osteoblasts by demonstrating and quantifying controlled seeding of primary osteoblasts, intercellular communications between live osteocytes in the trabecular bone matrix and seeded osteoblasts, and the maintenance of cell viability for long-term studies, and (2) examine the roles of two biochemical pathways, i.e., GJIC and PGE<sub>2</sub>, in functional trabecular bone response (bone formation and changes in apparent elastic modulus) under dynamic deformational loading.

## RESULTS AND DISCUSSION

### Establishment of Trabecular Bone Explant Co-Culture Model

To establish the trabecular bone explant co-culture model of *in situ* osteocytes and the seeded primary osteoblasts, bone marrow and all cells on the bone surface must be removed for a subsequent controlled seeding of osteoblasts. A PBS rinse-trypsinization-rinse technique was developed to facilitate the removal of all cells on the bone surface. The efficacy of this treatment was compared with that by the rinse only treatment (control). The trabecular bone explant cores were divided into two groups: (1) treatment and (2) control. The bone cores were first cleaned of bone marrow and most surface cells with sterile PBS using an Interplak water jet (WJ7B, ConAir, East Windsor, NJ). The treatment group was then treated with Trypsin-EDTA solution

for 5 min while the control group received regular culture medium. Bone cores in both groups were washed again with sterile PBS using the water jet. All cores were then cultured in six-well plates. The cores were harvested after one, two, and three weeks ( $n = 4$  for each group and time-point). At each time point, each core was vertically cut in half and stained using a live/dead cell viability stain. The trypsin treatment eliminated almost all surface cells while maintaining osteocyte viability (Fig. 1). Next, primary bovine osteoblasts were seeded into live trabecular bone explants using a custom-designed cell seeder.<sup>32</sup> The seeding efficiency and the final distribution of seeded osteoblasts in the 3D trabecular bone explants were examined. Two groups were compared in this study ( $n = 3$  for each group): (1) no seeding and (2) seeding of osteoblasts. Seeding efficiency was evaluated by the difference of cell numbers in medium before and immediately after seeding. The measurement indicated that an average of  $2 \times 10^5$  cells/core seeding efficiency was able to be achieved. The live/dead stain and fluorescence microscopy visually verified a uniform distribution of the seeded osteoblasts throughout the 3D bone cores 24 h after seeding (Fig. 2).

### Maintenance of Osteocyte Viability in Seeded Trabecular Bone Explants

To maintain osteocyte and osteoblast viability in seeded trabecular bone explants for long-term mechanobiology studies, a perfusion system was employed to allow a low-level medium perfusion at 0.01 ml/min through the bone explants.<sup>10</sup> Individual bone core explants with seeded osteoblasts were placed into perfusion chambers after 24 h of static culture. To verify the efficacy of the perfusion system on osteocyte viability, three experimental groups were compared ( $n = 4$ ): (1) initial cores after osteoblast seeding, (2) 2-week static culture, and (3) 2-week culture in the medium perfusion system. Live/dead stain and fluorescence microscopy showed that most of the osteocytes in the static culture group died after two weeks (Fig. 3a). On the contrary, the osteocytes in the trabecular bone cores in the perfusion group survived with a comparable viable osteocytes per bone area (OCY/BA) value to that of bone cores at initial day zero state (Figs. 3b and 3c). The OCY/BA value of the static culture group was significantly lower (less than 50%) than those of the initial and perfusion groups. Furthermore, the osteocyte viability in explants seeded with osteoblasts was extended and verified for up to 4 weeks in later experiments.

### GJIC of Osteocytes with Seeded Osteoblasts

To demonstrate the formation of functional GJIC between *in situ* osteocytes and the seeded osteoblasts, both qualitative fluorescence dye transfer techniques and a quantitative fluorescence flow cytometry technique were employed. First, the primary osteoblasts were labeled with green calcein-AM, a gap junction permeable fluorescent dye, prior to seeding in the trabecular explants.<sup>39</sup> The green calcein dye in the osteoblasts (shown as large green patches on the bone surface) was transferred to the neighboring osteocytes one day after seeding, indicating that the seeded osteoblasts established GJIC with the *in situ* osteocytes inside the trabecular bone matrix (Fig. 4a). The 3D reconstruction of confocal images indicated the spatial relationship between the osteoblasts on the bone surface and the small osteocytes underneath which had received the dye through intercellular transfer from the osteoblasts (Fig. 4b). Second, *in situ* osteocytes in trabecular explants were labeled with green calcein-AM, while osteoblasts were labeled with red DiI membrane dye prior to seeding. After a 1-week culture period, bone cells remained viable, and formation of functional GJIC between osteoblasts and osteocytes were confirmed (Figs. 4c–4e). The seeded osteoblasts appeared partially yellow in the combined overlay image as a result of overlap of the transferred green dye from *in situ* osteocytes to the osteoblasts labeled with the red membrane-bound dye. However, with the addition of a gap junction inhibitor, 18 $\alpha$ -glycyrrhetic acid (18 $\alpha$ -GA), in the culture medium, no apparent GJIC was observed, as the seeded osteoblasts remained red (Figs. 4f–4h). Therefore, these results collectively demonstrated the existence of functional GJICs between the seeded osteoblasts and osteocytes in the native explant environment. In addition, flow

cytometry was used to quantify the percentage of osteoblasts exhibiting GJIC with *in situ* live osteocytes embedded in the 3D bone matrix. As shown in Fig. 5, 8.8% of the non-labeled osteoblasts received calcein dye transfer from the *in situ* labeled osteocytes. With GJIC established in the live 3D trabecular bone explants, the role of GJIC on mechanotransduction in bone formation was further explored using this co-culture model.

### Dynamic Deformational Loading and Roles of GJIC

A 4-week co-culture study using a reversible gap junction inhibitor, 18 $\alpha$ -GA, was designed to study the role of GJIC in mechanotransduction between osteocytes and seeded osteoblasts in 3D trabecular bone explants. Trabecular bone explants seeded with osteoblasts were divided into four groups ( $n = 6$  for each group): (1) Vehicle + Loading (V + L), (2) Vehicle without loading (V), (3) 75  $\mu$ M 18 $\alpha$ -GA + Loading (18 $\alpha$ -GA + L), and (4) 75  $\mu$ M 18 $\alpha$ -GA without loading (18 $\alpha$ -GA). The bone explants were cultured in the perfusion system during the course of study except during mechanical loading. A sinusoidal dynamic axial deformational load was applied daily to groups 1 and 3 for the first three days of experiment using a custom built loading device with the explants immersed in culture medium. The sinusoidal, compressive, dynamic loading was applied at 1 Hz for 5 min with a 5 N preload and a load magnitude corresponded to an initial strain of 2400  $\mu$  $\epsilon$ .<sup>16</sup> The actual load on the specimen and the deformation of the bone cores were recorded simultaneously. Thus the apparent elastic modulus of individual explants, both at the beginning and at the end of the 4-week culture, was obtained. The elastic moduli of the explant cores ranged from 50 to 150 MPa. PGE<sub>2</sub> production for each specimen was measured 1 day before loading and every day during loading. The inhibitory effect of 18 $\alpha$ -GA on GJIC was confirmed with the calcein dye transfer as described previously (Fig. 6a). The toxicity of 18 $\alpha$ -GA appeared to be negligible for both osteocytes and osteoblasts, as assessed qualitatively by fluorescence confocal microscopy (Fig. 6a). Quantitative assessment further indicated that dynamic deformational loading and 18 $\alpha$ -GA had no significant effect on osteocyte viability (Fig. 6b). The OCY/BA value in this 4-week long-term experiment was not statistically different from the initial state or 2-week culture experiments. Interestingly, dynamic deformational loading did not significantly improve the viability of osteocytes in the explants (Fig. 6b). Our previous work, however, indicated that dynamic hydrostatic pressure improved osteocyte viability in long-term static culture.<sup>32</sup> One of the possible explanations for this discrepancy is the dramatically enhanced osteocyte viability due to medium perfusion in this study overshadowed the minor effects induced by mechanical loading. The OCY/BA of this study was  $\sim$ 800 osteocytes/mm<sup>2</sup> throughout the entire experiment, while the previous study using dynamic hydrostatic pressure was only able to maintain  $\sim$ 500 osteocytes/mm<sup>2</sup> for 8 days before dramatic decline.

Dynamic deformational loading induced significantly higher PGE<sub>2</sub> release from the explant system compared to the non-loaded culture group, and this loading-induced PGE<sub>2</sub> release was significantly attenuated by GJIC inhibition using 18 $\alpha$ -GA (Fig. 7a). While the high level of PGE<sub>2</sub> release by mechanical loading was sustained in the second and third day of culture, the continuous GJIC inhibition abolished the loading-enhanced PGE<sub>2</sub> release after the first day. This result is consistent with previous findings where mechanical loading-induced secretion of PGE<sub>2</sub> in osteocytes was shown to occur via Cx43 hemichannels.<sup>31</sup> The present 3D explant co-culture model confirmed the intimate interaction between GJIC and PGE<sub>2</sub> release. Mechanical loading in the first three days also significantly increased bone formation, as indicated by the osteoid surface per bone surface (OS/BS) percentage after 4 weeks (Fig. 7b). The GJIC inhibition significantly reduced, but did not completely eliminate, the loading-induced enhancement in bone formation (Fig. 7b). Dynamic deformational loading generated a significantly higher increase in apparent elastic modulus of trabecular bone cores compared to the non-loaded groups (Fig. 7c). This loading-induced increase in the apparent elastic modulus was negated by GJIC inhibition. Therefore, the continuous inhibition of GJIC in

osteocytes and/or osteoblasts can diminish the loading-enhanced secretion of PGE<sub>2</sub>, the loading-induced increase in bone formation, and the loading-induced increase in apparent elastic modulus. The intriguing effect on PGE<sub>2</sub> release implicated the critical role of PGE<sub>2</sub> in bone mechanotransduction, which was further addressed in the following study below.

### Dynamic Deformational Loading and Roles of PGE<sub>2</sub>

To investigate the role of mechanical loading on PGE<sub>2</sub> release, bone formation and apparent elastic modulus in trabecular bone explants seeded with osteoblasts, a 4-week experiment was carried out with NS-398 treatment, as NS-398 selectively inhibits COX-2 enzyme activity.<sup>27</sup> PGE<sub>2</sub> is mainly produced via the COX-2 pathway in bone cells subjected to mechanical loading. Thus inhibition of COX-2 enzyme activity can significantly inhibit the loading-induced PGE<sub>2</sub> release in bone cells. Bone explants were divided into four groups ( $n = 6$  for each group): (1) Vehicle + Loading (V + L), (2) Vehicle without loading (V), (3) 10  $\mu$ M NS-398 + Loading (NS-398 + L), and (4) 10  $\mu$ M NS-398 without loading (NS-398). The loading and measurement protocols were the same as described in the previous GJIC study. With either mechanical loading or COX-2 inhibition, osteocyte viability was maintained in this 4-week experiment, similar to the GJIC inhibition study (Fig. 8a). The dynamic deformational loading elevated PGE<sub>2</sub> release significantly, especially on day 1, while PGE<sub>2</sub> release in the unloaded (V) group gradually declined (Fig. 8b). This trend is consistent with those reported in previous studies.<sup>37</sup> The COX-2 inhibition by NS-398 blocked the PGE<sub>2</sub> production/release. Again, applying dynamic deformational loading for only 3 days resulted in a significant increase in bone formation after four weeks, as evident by the increase in OS/BS (Fig. 8c). However, the effect of mechanical loading on bone formation was completely abolished when NS-398 was present. A significant increase in apparent elastic modulus of trabecular bone explants was observed after four weeks, and COX-2 inhibition completely eliminated any increase in apparent elastic modulus (Fig. 8d). Previous *in vivo* and *in vitro* studies have demonstrated that either osteocytes or osteoblasts release PGE<sub>2</sub> upon mechanical stimulation.<sup>3-5,11-14,23,38</sup> However, *in vitro* studies of the mechanical stimulation of osteoblasts or osteocytes have not shown that the mechanically stimulated PGE<sub>2</sub> release can lead to eventual increase of bone formation.<sup>26</sup> Using our 4-week co-culture model with live trabecular bone cores, we have successfully linked the early mechanically induced PGE<sub>2</sub> release with the bone formation and changes in apparent elastic modulus.

In summary, a unique co-culture trabecular bone explant model for studying mechanotransduction of osteocytes and osteoblasts has been developed and established. This model allows live osteocytes in their native mineralized extracellular matrix to interact in a controlled manner with osteoblasts in their natural spatial context. Low-level medium perfusion was sufficient to meet the nutrient requirements of both osteocytes *in situ* and osteoblasts on the bone surface. The live osteocytes that resided inside the mineralized bone tissue were able to establish physical contact and GJIC with seeded osteoblasts. Using this model, dynamic deformational load can be applied to 3D trabecular bone samples. In light of this loading system, the roles of GJIC and PGE<sub>2</sub> release in mechanotransduction in bone have been quantified in terms of functional bone adaptation (bone formation and changes in apparent elastic modulus) *in vitro*, which have not been demonstrated in previous *in vitro* studies. Results from these two studies showed that dynamic deformational loading can induce PGE<sub>2</sub> release from bone cells and thereby increase the bone formation and apparent elastic modulus of bone explants. The inhibition of GJIC and PGE<sub>2</sub> release significantly attenuated or abolished the effects induced by mechanical loading.

It should be emphasized that only two types of cells are present in this model: live *in situ* osteocytes and seeded osteoblasts. Therefore, the roles of GJIC and PGE<sub>2</sub> in mechanotransduction between osteocytes and osteoblasts can be demonstrated quantitatively

in this explant model. *Ex vivo* culture of whole trabecular explants (including bone marrow) is also being pursued by several other groups.<sup>16,17,25</sup> However, the uncontrollable components, such as dying or dead blood vessels, red/white blood cells, and nerves, may complicate the search for clear delineations of the role of OCY-OB interactions and of particular biochemical pathways in mechanotransduction in bone. It is now known that both the vascular and nervous systems have significant influences on bone function,<sup>7,33</sup> but it is difficult to control either parameter in an *in vitro* trabecular bone explant model containing disrupted remnants of both vasculature elements and nerves. The advantage of this particular *in vitro* trabecular bone explant model is not its ability to completely re-capitulate the *in vivo* system, but rather to simplify the *in vivo* system sufficiently to investigate specific mechanotransduction pathways. For example, a selective inhibition of the GJIC or PGE<sub>2</sub> pathways in osteoblasts ONLY without affecting the osteocytes can be achieved in our system with RNAi-based knockdown in the osteoblasts. On the other hand, tissue-specific knockout mouse technology can inhibit either *both osteocytes and osteoblasts or only osteocytes*. It is this unique and novel feature of this 3D trabecular bone explant co-culture model that will fill in the critical gap in the lack of physiologically relevant model systems for elucidating the role of osteocytes as a mechano-sensor and how osteocytes transmit signals to regulate osteoblast functions.

## MATERIALS AND METHODS

### Chemicals

Minimum essential alpha medium ( $\alpha$ -MEM), calcein-AM, ethidium homodimer-1, and DiI, were obtained from Invitrogen (Carlsbad, CA). Fetal bovine serum (FBS), penicillin/streptomycin (P/S), trypsin-EDTA, dexamethasone, ascorbic acid,  $\beta$ -glycerophosphate, DMSO, and 18 $\alpha$ -glycyrrhetic acid were obtained from Sigma-Aldrich (St. Louis, MO). NS-398 was obtained from Cayman Chemicals (Ann Arbor, MI).

### Trabecular Bone Explant Harvesting and Controlled Seeding of OBs

Trabecular bone cores were harvested from the epiphysis of fresh tarsal-metatarsal joints of 3-month-old calves (Green Village Packing Company, Green Village, NJ). Prior to harvesting, the entire joints were skinned and sterilized by a detergent solution followed by 70% ethanol. Under sterile conditions and constant irrigation with phosphate buffered saline (PBS), cylindrical trabecular bone cores ( $\phi = 7$  mm and  $h = 7$  mm) were harvested using a diamond tipped coring tool (Starlite Industries, Rosemont, PA) and an Isomet low-speed saw (Buehler, Lake Bluff, IL). The cores were obtained in regions beyond 7 mm from the articular cartilage. All cores were cleaned with sterile PBS jet (ConAir, East Windsor, NJ), treated with trypsin for 5 min, and repeated PBS jet rinsing in order to remove bone marrow and cells on the bone surface.

Primary osteoblasts were obtained from trabecular bone chips harvested from the same region as the bone cores. Trabecular bone cores were obtained as described above, minced into small chips in Hank's buffered salt solution, and rinsed several times to remove bone marrow. The bone chips were then transferred to cell culture dishes with  $\alpha$ -MEM supplemented with 10% FBS and 1% P/S. After approximately 7 days culture, the bone chips were transferred to a new culture dish where the second batch of osteoblasts was allowed to migrate out for approximately another 1–2 weeks at which time the osteoblasts were used. The first batch of cells that migrated out of the bone chips were discarded, as they were of a more heterogeneous population. Using a custom-designed cell seeder, cleaned bone cores were seeded the day after harvest in the cell seeder for 1 h.<sup>32</sup> To ensure primary osteoblast attachment, all cores were individually cultured statically for 24 h with "osteogenic medium",  $\alpha$ -MEM supplemented with 10% FBS, 1% P/S,

100 nmol/L dexamethasone, 0.2 mmol/L ascorbic acid and 10 mmol/L  $\beta$ -glycerophosphate, before transferring to the medium perfusion system.

### Medium Perfusion System

A perfusion system was built to achieve low-level osteogenic medium perfusion of 0.01 ml/min through the co-culture explants to maintain the long-term cell viability.<sup>10</sup> The system consisted of custom-built polycarbonate chambers to hold the bone cores, Pharmed® tubing, and a multi-channel precision fluid pump (Manostat Carter, Barrington, IL). For the perfusion medium to pass through the co-culture explants but not around them, explants were held inside the chambers and sealed in place with o-rings above and below them.<sup>6</sup>

### Load Controlled Dynamic Deformational Loading System

To deliver precise dynamic uniaxial deformational loading on bone cores under sterile conditions, a bench-top mechanical loading system was designed and built for usage in a laminar flow hood. The loading device consisted of a linear voice coil actuator (LA25-42-000A, BEI Kimco Magnetics Division, Vista, CA) that drove the loading tip, a submersible load transducer (Q11998, FUTEK, Irvine, CA) that recorded the load applied to the sample, and an Eddy current proximity sensor (KD-2300TM, Kaman Measuring Systems, Colorado Springs, CO) that measured the actuator displacement. The feedback control units consisted of a LabVIEW® program (Version 7.1), a servo motion controller (FW-7344), a universal motion interface (UMI-7764) (all from the National Instruments Corporation, Austin, TX), and a brush type pulse-width modulation servo amplifier (C50A1B, Advanced Motion Controls, Camarillo, CA), and a proportion-integral-derivative (PID) controller to achieve load feedback control of the loading system. The loading and displacement history were recorded at 30 Hz using the LabView program.

### GJIC or PGE<sub>2</sub> Production Inhibition Studies

Osteogenic medium was supplemented with 75  $\mu$ M 18 $\alpha$ -GA during the duration of the experiment for GJIC inhibition studies.<sup>36,39</sup> Osteogenic medium was supplemented with 10  $\mu$ M NS-398 for PGE<sub>2</sub> blocking experiments.<sup>4</sup> Since both chemicals were first dissolved in DMSO, a vehicle control group was included with 0.05% (v/v) DMSO in medium during experiments.

### PGE<sub>2</sub> Release Quantification

In order to verify the blocking effects of NS-398 and to investigate the change of mechanically induced PGE<sub>2</sub> release, culture medium in the perfusion system was collected at four different time points: baseline (before loading) and 2 h after first, second, and third batch of mechanical loadings ( $n = 6$  each). Collected sample medium was centrifuged, and the supernatants were stored at  $-80$  °C until the day of analysis. PGE<sub>2</sub> levels in the medium were measured using a commercial PGE<sub>2</sub> EIA kit (Cayman Chemical, Ann Arbor, MI) according to manufacturer's instructions.

### Quantitative Confirmation of GJIC by Flow Cytometry

Flow cytometry was used to quantify the percentage of osteoblasts exhibiting GJIC with *in situ* live osteocytes embedded in the 3D bone matrix. The osteoblasts on the bone explant surface were removed by trypsinization. The percentage of osteoblasts with intracellular calcein dye uptake was quantified using a flow cytometer (BD LSR II System) with an excitation wavelength of 488 nm and a 515–545 nm emission filter. A total of 30,000–50,000 cells were quantified for each bone core at a measurement rate of 300–400 cells/s. Appropriate gates were set to identify autofluorescence from calcein in Cell Quest Pro software (Becton-

Dickinson). In addition, viable cells were selected by setting gate for forward light scatter at 488 nm.

### Bone Histology

Bone cores were cut vertically into two halves after the prescribed experiments for the qualitative assessment of cell viability by live/dead staining and confocal microscopic imaging. The half sample was further fixed in 10% neutral buffered formalin to evaluate the osteoid formation by bone histomorphometry. In brief, the fixed specimens were embedded in plastic and sectioned at 8  $\mu\text{m}$  thickness. Non-consecutive sections were stained with Goldner Trichrome's dye to show osteoid in red and bone tissue in green. Osteoid surface per bone surface (OS/BS) was measured to investigate the osteogenic activities in the explants.

The other half of each sample was decalcified in buffered formic acid, paraffin embedded, and sectioned at 8  $\mu\text{m}$  thickness. Non-consecutive sections were stained with H&E dyes to obtain OCY/BA. Osteocytes in lacunae with intact (round to oval), darkly stained, and smooth-edged nucleus were considered alive, while those with condensed, fragmented, or pale indistinct nuclei were considered dead. An area of 400  $\mu\text{m}$  wide and 4000  $\mu\text{m}$  tall in the center of each section was analyzed under a light microscope with a 20 $\times$  objective, using the bone histomorphometry software OsteoMeasure (Osteometrics, GA).

### Statistics

Osteocyte viability, osteoid formation, and percentage change of apparent elastic modulus over 4 weeks of each group were analyzed by two-way analysis of variance (ANOVA) with an LSD *post hoc* test (SYSTAT, Point Richmond, CA). The PGE<sub>2</sub> secretion for each group was analyzed at each time point using two-way ANOVA with a LSD *post hoc* test.  $p < 0.05$  was considered statistically significant.

### Acknowledgments

We would like to thank Ms. Jiasi Chen for her assistance in histology. This work was supported by NIH grant R21 AR052417 (X. Edward Guo).

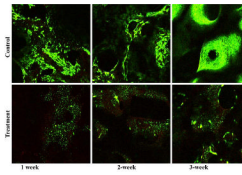
### REFERENCES

1. Ajubi NE, Klein-Nulend J, Nijweide PJ, Vrijheid-Lammers T, Alblas MJ, Burger EH. Pulsating fluid flow increases prostaglandin production by cultured chicken osteocytes—a cytoskeleton-dependent process. *Biochem. Biophys. Res. Commun* 1996;225:62–68. [PubMed: 8769095]
2. Alford AI, Jacobs CR, Donahue HJ. Oscillating fluid flow regulates gap junction communication in osteocytic MLO-Y4 cells by an ERK1/2 MAP kinase-dependent mechanism. *Bone* 2003;33:64–70. [PubMed: 12919700]
3. Bakker AD, Joldersma M, Klein-Nulend J, Burger EH. Interactive effects of PTH and mechanical stress on nitric oxide and PGE<sub>2</sub> production by primary mouse osteoblastic cells. *Am. J. Physiol.-Endocrinol. Metab* 2003;285:E608–E613. [PubMed: 12746215]
4. Bakker AD, Klein-Nulend J, Burger EH. Mechanotransduction in bone cells proceeds via activation of COX-2, but not COX-1. *Biochem. Biophys. Res. Commun* 2003;305:677–683. [PubMed: 12763047]
5. Bakker AD, Soejima K, Klein-Nulend J, Burger EH. The production of nitric oxide and prostaglandin E<sub>2</sub> by primary bone cells is shear stress dependent. *J. Biomech* 2001;34:671–677. [PubMed: 11311708]
6. Bancroft GN, Sikavitsas VI, van den Dolder J, Sheffield TL, Ambrose CG, Jansen JA, Mikos AG. Fluid flow increases mineralized matrix deposition in 3D perfusion culture of marrow stromal osteoblasts in a dose-dependent manner. *Proc. Natl Acad. Sci. USA* 2002;99:12600–12605. [PubMed: 12242339]



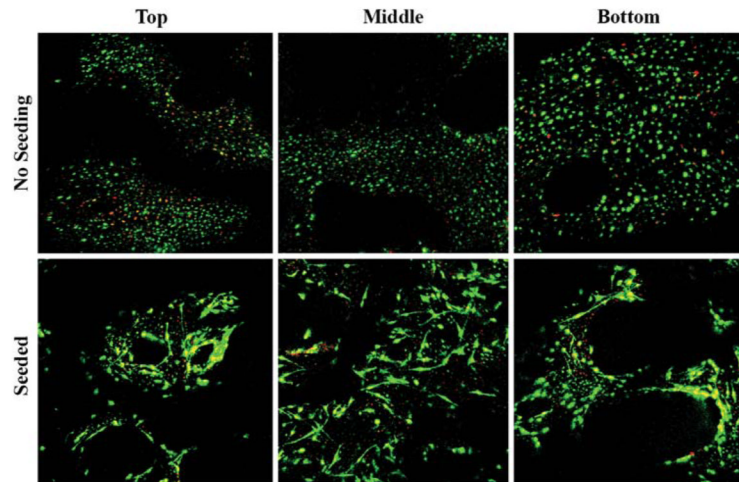
7. Brandi ML, Collin-Osdoby P. Vascular biology and the skeleton. *J. Bone Miner. Res* 2006;21:183–192. [PubMed: 16418774]
8. Burger EH, Klein-Nulend J. Mechanotransduction in bone—role of the lacuno-canalicular network. *FASEB J* 1999;13:S101–S112. [PubMed: 10352151]
9. Burger EH, Klein-Nulend J, Veldhuizen JP. Modulation of osteogenesis in fetal bone rudiments by mechanical stress in vitro. *J. Biomech* 1991;24(Suppl. 1):101–109. [PubMed: 1791171]
10. Cartmell SH, Porter BD, Garcia AJ, Guldberg RE. Effects of medium perfusion rate on cell-seeded three-dimensional bone constructs in vitro. *Tissue Eng* 2003;9:1197–1203. [PubMed: 14670107]
11. Chambers TJ, Chow JW, Fox SW, Jagger CJ, Lean JM. The role of prostaglandins and nitric oxide in the response of bone to mechanical stimulation. *Adv. Exp. Med. Biol* 1997;433:295–298. [PubMed: 9561155]
12. Chambers TJ, Fox S, Jagger CJ, Lean JM, Chow JW. The role of prostaglandins and nitric oxide in the response of bone to mechanical forces. *Osteoarthritis Cartilage* 1999;7:422–423. [PubMed: 10419787]
13. Cherian PP, Siller-Jackson AJ, Gu S, Wang X, Bonewald LF, Sprague E, Jiang JX. Mechanical strain opens connexin 43 hemichannels in osteocytes: a novel mechanism for the release of prostaglandin. *Mol. Biol. Cell* 2005;16:3100–3106. [PubMed: 15843434]
14. Chow JW. Role of nitric oxide and prostaglandins in the bone formation response to mechanical loading. *Exerc. Sport Sci. Rev* 2000;28:185–188. [PubMed: 11064853]
15. Dallas SL, Zaman G, Pead MJ, Lanyon LE. Early strain-related changes in cultured embryonic chick tibiotarsi parallel those associated with adaptive modeling in vivo. *J. Bone Miner. Res* 1993;8:251–259. [PubMed: 7681245]
16. David V, Guignandon A, Martin A, Malaval L, Lafage-Proust MH, Rattner A, Mann V, Noble B, Jones DB, Vico L. *Ex vivo* bone formation in bovine trabecular bone cultured in a dynamic 3D bioreactor is enhanced by compressive mechanical strain. *Tissue Eng. Part A* 2008;14:117–126. [PubMed: 18333810]
17. Davies CM, Jones DB, Stoddart MJ, Koller K, Smith E, Archer CW, Richards RG. Mechanically loaded *ex vivo* bone culture system ‘Zetos’: systems and culture preparation. *Eur. Cell Mater* 2006;11:57–75. discussion 75. [PubMed: 16612792]
18. El-Haj AJ, Minter SL, Rawlinson SC, Suswillo R, Lanyon LE. Cellular responses to mechanical loading in vitro. *J. Bone Miner. Res* 1990;5:923–932. [PubMed: 1704173]
19. Genet DC, Kephart CJ, Zhang Y, Yellowley CE, Donahue HJ. Oscillating fluid flow activation of gap junction hemichannels induces ATP release from MLO-Y4 osteocytes. *J. Cell. Physiol* 2007;212:207–214. [PubMed: 17301958]
20. Hoffler CE, Hankenson KD, Miller JD, Bilkhu SK, Goldstein SA. Novel explant model to study mechanotransduction and cell-cell communication. *J. Orthop. Res* 2006;24:1687–1698. [PubMed: 16788985]
21. Hung CT, Allen FD, Pollack SR, Brighton CT. Intracellular  $\text{Ca}^{2+}$  stores and extracellular  $\text{Ca}^{2+}$  are required in the  $[\text{Ca}^{2+}]_i$  response of bone cells experiencing fluid flow. *J. Biomech* 1996;29(11):1403–1409. [PubMed: 8894920]
22. Jacobs CR, Yellowley CE, Davis BR, Zhou Z, Cimbala JM, Donahue HJ. Differential effect of steady versus oscillating flow on bone cells. *J. Biomech* 1998;31:969–976. [PubMed: 9880053]
23. Jiang JX, Siller-Jackson AJ, Burra S. Roles of gap junctions and hemichannels in bone cell functions and in signal transmission of mechanical stress. *Front. Biosci* 2007;12:1450–1462. [PubMed: 17127393]
24. Malone AM, Anderson CT, Tummala P, Kwon RY, Johnston TR, Stearns T, Jacobs CR. Primary cilia mediate mechanosensing in bone cells by a calcium-independent mechanism. *Proc. Natl Acad. Sci. USA* 2007;104:13325–13330. [PubMed: 17673554]
25. Mann V, Huber C, Kogianni G, Jones D, Noble B. The influence of mechanical stimulation on osteocyte apoptosis and bone viability in human trabecular bone. *J. Musculoskelet. Neuronal Interact* 2006;6:408–417. [PubMed: 17185839]
26. Nauman EA, Satcher RL, Keaveny TM, Halloran BP, Bikle DD. Osteoblasts respond to pulsatile fluid flow with short-term increases in  $\text{PGE}_2$  but no change in mineralization. *J. Appl. Physiol* 2001;90:1849–1854. [PubMed: 11299276]

27. Norvell SM, Ponik SM, Bowen DK, Gerard R, Pavalko FM. Fluid shear stress induction of COX-2 protein and prostaglandin release in cultured MC3T3-E1 osteoblasts does not require intact microfilaments or microtubules. *J. Appl. Physiol* 2004;96:957–966. [PubMed: 14617531]
28. Pitsillides AA, Rawlinson SC, Suswillo RF, Bourrin S, Zaman G, Lanyon LE. Mechanical strain-induced NO production by bone cells: a possible role in adaptive bone (re)modeling? *FASEB J* 1995;9:1614–1622. [PubMed: 8529841]
29. Rawlinson SC, El-Haj AJ, Minter SL, Tavares IA, Bennett A, Lanyon LE. Loading-related increases in prostaglandin production in cores of adult canine cancellous bone in vitro: a role for prostacyclin in adaptive bone remodeling? *J. Bone Miner. Res* 1991;6:1345–1351. [PubMed: 1724342]
30. Rawlinson SC, Wheeler-Jones CP, Lanyon LE. Arachidonic acid for loading induced prostacyclin and prostaglandin E<sub>2</sub> release from osteoblasts and osteocytes is derived from the activities of different forms of phospholipase A<sub>2</sub>. *Bone* 2000;27:241–247. [PubMed: 10913917]
31. Siller-Jackson AJ, Burra S, Gu S, Xia X, Bonewald LF, Sprague E, Jiang JX. Adaptation of connexin 43-hemichannel prostaglandin release to mechanical loading. *J. Biol. Chem* 2008;283:26374–26382. [PubMed: 18676366]
32. Takai E, Mauck RL, Hung CT, Guo XE. Osteocyte viability and regulation of osteoblast function in a 3D trabecular bone explant under dynamic hydrostatic pressure. *J. Bone Miner. Res* 2004;19:1403–1410. [PubMed: 15312240]
33. Takeda S, Karsenty G. Molecular bases of the sympathetic regulation of bone mass. *Bone* 2008;42:837–840. [PubMed: 18295563]
34. Tan SD, Kuijpers-Jagtman AM, Semeins CM, Bronckers AL, Maltha JC, Von den Hoff JW, Everts V, Klein-Nulend J. Fluid shear stress inhibits TNF $\alpha$ -induced osteocyte apoptosis. *J. Dent. Res* 2006;85:905–909. [PubMed: 16998129]
35. Tatsumi S, Ishii K, Amizuka N, Li M, Kobayashi T, Kohno K, Ito M, Takeshita S, Ikeda K. Targeted ablation of osteocytes induces osteoporosis with defective mechanotransduction. *Cell Metab* 2007;5:464–475. [PubMed: 17550781]
36. Taylor AF, Saunders MM, Shingle DL, Cimbala JM, Zhou Z, Donahue HJ. Mechanically stimulated osteocytes regulate osteoblastic activity via gap junctions. *Am. J. Physiol. Cell Physiol* 2007;292:C545–C552. [PubMed: 16885390]
37. Vance J, Galley S, Liu DF, Donahue SW. Mechanical stimulation of MC3T3 osteoblastic cells in a bone tissue-engineering bioreactor enhances prostaglandin E<sub>2</sub> release. *Tissue Eng* 2005;11:1832–1839. [PubMed: 16411829]
38. Watanuki M, Sakai A, Sakata T, Tsurukami H, Miwa M, Uchida Y, Watanabe K, Ikeda K, Nakamura T. Role of inducible nitric oxide synthase in skeletal adaptation to acute increases in mechanical loading. *J. Bone Miner. Res* 2002;17:1015–1025. [PubMed: 12054156]
39. Yellowley CE, Li Z, Zhou Z, Jacobs CR, Donahue HJ. Functional gap junctions between osteocytic and osteoblastic cells. *J. Bone Miner. Res* 2000;15:209–217. [PubMed: 10703922]
40. Zaman G, Dallas SL, Lanyon LE. Cultured embryonic bone shafts show osteogenic responses to mechanical loading. *Calcif. Tissue Int* 1992;51:132–136. [PubMed: 1422952]



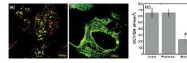
**FIGURE 1.**

Live/dead viability stains at different time points focused on the center region of vertical sections of explants: top = control and bottom = rinse-trypsinization-rinse treatment. A minimal number of surface cells were present even after 3 weeks culture in the treatment group while the surface of control samples was populated with cells.

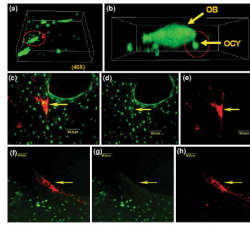


**FIGURE 2.**

Micrographs of osteoblast distributions at three different regions of the explant (top, middle, and bottom) after controlled seeding using the custom-designed cell seeder. As compared with the group with no osteoblast seeding, the seeded osteoblasts were evenly distributed across the entire 3D trabecular bone core.

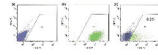
**FIGURE 3.**

Effects of medium perfusion on cell viability. (a) In a 2-week comparison experiment, most osteocytes in the static culture group died, shown as red dots in the image. (b) The osteocytes in the perfusion group survived. (c) Quantitative analysis showed that the co-cultured trabecular explants in medium perfusion system had similar viable osteocytes per bone area (OCY/BA) to the sample at initial state, both are significantly higher than the explants in static culture for 2 weeks (# vs. all other groups  $p < 0.05$ ).

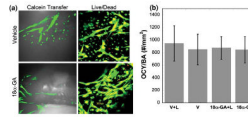


**FIGURE 4.**

GJIC between OCYs and OBs: (a) a 3D reconstructed image of a 1-day-culture sample showing the seeded osteoblasts (OBs) (large patch-like cells) stained in green and its surrounding smaller osteocytes (OCYs); (b) a close-up of the circled region in the left image showing gap junction between an OB and an OCY; (c) OB (arrow) appearing in yellow indicates the transfer of calcein from *in situ* OCY (overlay); (d) the green channel image clearly shows both the *in situ* OCY and the cytosol of OB stained in green; (e) the red channel image shows the OBs membrane in red; (f) with gap junction inhibited, a pure red OB indicates no green dye transfer from *in situ* OCYs; (g & h) absence of green at the position of OBs cytosol in both green and red channel images.

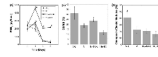
**FIGURE 5.**

Quantitative assessment of GJIC. (a) Non-labeled osteoblasts and (b) calcein-labeled osteoblasts were used for properly setting up the gate P3 to exclude the autofluorescent osteoblasts from calcein-labeled bovine osteoblasts. (c) 8.8% of osteoblasts exhibited GJIC with *in situ* osteocytes.

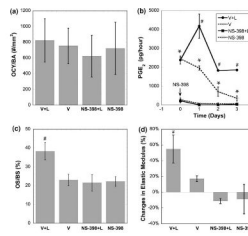
**FIGURE 6.**

Explant osteocyte viability under mechanical loading and GJIC inhibition. (a) Calcein transfer, an indication of functional GJIC, was observed in the vehicle control sample but not in the presence of gap junction inhibitor (18 $\alpha$ -GA). Live-dead stain showed the majority of cells remained viable for all groups. (b) The co-cultured trabecular explants in all groups had similar viable osteocytes per bone area (OCY/BA) values.



**FIGURE 7.**

The role of GJIC in bone mechanotransduction. (a) PGE<sub>2</sub> release during 3-day dynamic deformational loading (loading at first, second, and third day, \* vs. 18α-GA  $p < 0.05$ ; # vs. all other groups  $p < 0.05$ ). (b) Osteoid surface per bone surface (OS/BS) in explants after the 4-week experiment (\* vs. all other groups  $p < 0.05$ ; # vs. 18α-GA  $p < 0.05$ ). (c) Changes in apparent elastic modulus of bone explants after 4-weeks culture (# vs. all other groups  $p < 0.05$ ). Error bars are standard deviation.

**FIGURE 8.**

The role of PGE<sub>2</sub> release on bone mechanotransduction. (a) Osteocyte viability after the 4-week experiment with NS-398 treatment. (b) PGE<sub>2</sub> release during 3-day dynamic deformational loading (loading at first, second, and third day, \* vs. NS-398 groups  $p < 0.05$ ; # vs. all other groups  $p < 0.05$ ). (c) Osteoid surface per bone surface in explants after the 4-week experiment (# vs. all other groups  $p < 0.05$ ). (d) Changes in apparent elastic modulus of bone explants after 4-week culture (# vs. all other groups  $p < 0.05$ ). Error bars are standard deviations.